A NOVEL RECONFIGURABLE TRI-MODE RESONATOR AND ITS APPLICATION TO BANDPASS FILTER

by

Jun CHENG, Xiu-Shan LIU, and Qin ZHANG *

School of Electronics and Information, Guangdong Polytechnic Normal University, Guangzhou, China

Original scientific paper
https://doi.org/10.2298/TSCI2202131C

A reconfigurable tri-mode resonator and its application to tri-band bandpass filter have been demonstrated. The proposed filter exhibits 32.8% fractional tuning range of the first passband from 1.12-1.56 GHz and 12.73% of the third passband from 2.50-2.84 GHz, and a fixed second passband at 2 GHz, respectively. The first and third frequency passbands can be tuned independently without interfering with each other. Especially, the filter uses a hybrid technique of lumped inductors and microstrip lines, resulting in a very compact mechanical size of 0.12 $\lambda_g \times 0.08\ \lambda_g$, where λ_g is the guided wavelength on the substrate at the central of the first passband frequency. The measured results agree well with the simulated ones.

Key words: *bandpass filter, compact size, tri-band, reconfigurable*

Introduction

With the rapid development of modern communication technology, the research of reconfigurable filters is becoming more and more popular due to their good compatibility and low cost. In recent years, some different types of reconfigurable filters have been developed. In Chen *et al.* [1], a reconfigurable bandpass filter (BPF) with constant absolute bandwidth and independently controlled passbands is proposed. In Sedighi *et al.* [2], a novel dual-band tunable filter is designed to support multi-standard applications. A balanced dual-band BPF is proposed in [3], which has independently tunable differential mode frequencies. A dual-mode dual-band filter is presented in [4], which is based on half-mode substrate integrated waveguide technology. However, all the references are focused on dual-band reconfigurable filters, which cannot meet the requirements of the communication systems that need more passbands. A tri-band BPF is proposed in [5], in which novel resonators are used to implement a BPF with tunable lower passband, but it has only one tunable frequency band. Tunable tri-band BPF are also presented in [6], but which also has only one tunable passband. In Kingsly *et al.* [7], through the combination of pin diodes, the filter can work in a series of two-band or three-band states, but it can only provide discrete center frequencies and cannot achieve continuous tuning. Compact tri-band filter with three tunable passbands is proposed in [8]. However, due to its coupling structure, it has a larger mechanical size and does not meet the requirements of miniaturization. Furthermore, its insertion loss is not good during the tuning range. In [9-15], the authors proposed a variety of multi-band BPF, some of which are excel-

* Corresponding author, e-mail: zhangqin1100@outlook.com

lent in performance. However, they are all fixed-bands filters and can not be tuned. In this paper, a novel tri-band tunable resonator and corresponding filter are presented, The proposed filter has two tunable frequency bands and one fixed frequency band. The hybrid technology of lumped circuit and microstrip line is applied in this design, which can greatly reduce the size of the filter.

Discussion on the basic resonator

Figure 1 shows the structure of the basic tri-band resonator. The pin diode can control the resonator to work in dual-band or tri-band. In this section, we only discuss the resonator working in tri-band mode. Since the proposed structure is symmetrical, the even- and odd--mode analysis method can be applied to obtain the resonant frequencies.

For odd-mode excitation, as shown in fig. 2(a). The first odd-mode resonant frequency can be obtained as:

$$f_{\mathrm{odd}} = \frac{(2n-1)c}{2L_1\sqrt{\varepsilon_{\mathrm{eff}}}} \tag{1}$$

where $\varepsilon_{\mathrm{ff}}$ denotes the effective dielectric constant of the substrate and c is the speed of light in free space.

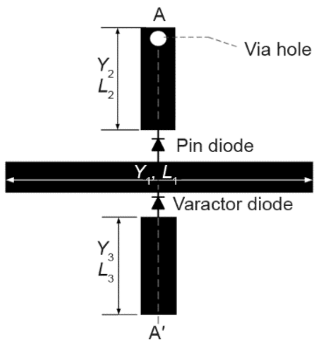

Figure 1. Configuration of the basic resonator

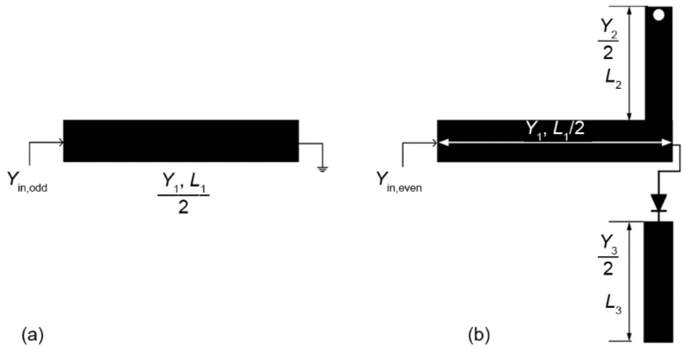

Figure 2. (a) Odd-mode equivalent circuit and (b) even-mode equivalent circuit

For the short stub resonator shown in fig. 3(a), the input impedance can be expressed:

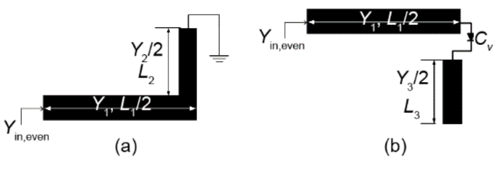

Figure 3. (a) Part 1 of even-mode equivalent circuit and (b) part 2 of even-mode equivalent circuit

$$Y_{\mathrm{in,even1}} = -jY_1 \frac{Y_2 - 2Y_1 \tan\dfrac{\theta_1}{2}\tan\theta_2}{2Y_1\tan\theta_2 + Y_2\tan\dfrac{\theta_1}{2}} \tag{2}$$

where $\theta_i = \beta L_i$ denotes the electric length of the certain microstrip line. From the resonance condition of $\mathrm{Im}[Y_{\mathrm{in,even1}}] = 0$, the first resonant frequency of this stub can be obtained:

$$f_{\mathrm{even1}} = \frac{(2n-1)c}{(2L_1 + 4L_2)\sqrt{\varepsilon_{\mathrm{eff}}}} \tag{3}$$

For the open stub connected with a varactor diode, as shown in fig. 3(b), the input impedance can be deduced:

$$Y_{\text{in,even}2} = Y_1 \frac{Y_s + jY_1 \tan\dfrac{\theta_1}{2}}{Y_1 + jY_s \tan\dfrac{\theta_1}{2}} \tag{4}$$

where

$$Y_s = \frac{j\omega C_\text{v}\, j\dfrac{Y_3}{2}\tan\theta_3}{j\omega C_\text{v} + j\dfrac{Y_3}{2}\tan\theta_3} \tag{5}$$

$$\theta_i = \beta L_i = \frac{2\pi f}{v_p} L_i \tag{6}$$

where C_v is the capacitance of the varactor diode connected at the center of the transmission line and the open stub. For the resonance condition of $\text{Im}[Y_{\text{in,even}2}] = 0$, the resonant frequency can be determined:

$$Y_3 \tan\left(\frac{\pi f_{\text{even}2} L_3}{v_p}\right) + 2Y_1 \tan\left(\frac{\pi f_{\text{even}2} L_1}{v_p}\right) = \frac{-Y_1 Y_3 \tan\left(\dfrac{\pi f_{\text{even}2} L_3}{v_p}\right)\tan\left(\dfrac{\pi f_{\text{even}2} L_1}{v_p}\right)}{2\pi f C_\text{v}} \tag{7}$$

Analysis of the proposed resonator

The basic tri-band resonator has some performance, but it can be optimized. The inspiration for optimization comes from eq. (7). By analyzing eq. (7), it can be found that the length of the microstrip line L_3 can be any value. So, we can try to reduce the length of the microstrip line L_3 to zero. Thus, for the open stub connected with a varactor diode, as shown in fig. 3(b), it can be simplified to consist of only one varactor diode and without any stub. This design can greatly reduce the mechanical length of this branch.

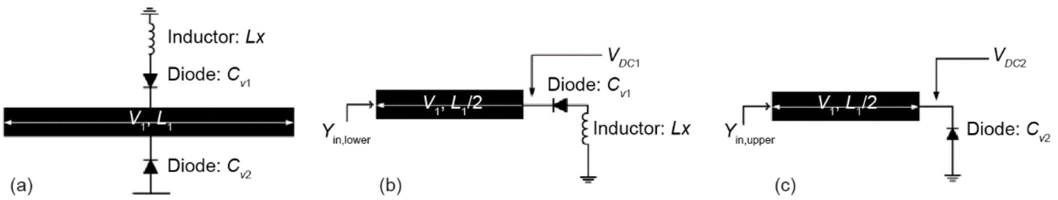

Figure 4. Configuration of the proposed resonator

According to the previous ideas, the optimized open stub resonator is shown as fig. 4(c). The input impedance of this optimized branch can be expressed:

$$Y_{\text{in,upper}} = Y_1 \frac{j\omega C_{\text{v}2} + jY_1 \tan\dfrac{\theta_1}{2}}{Y_1 + jj\omega C_{\text{v}2} \tan\dfrac{\theta_1}{2}} \tag{8}$$

For the resonance condition of $\mathrm{Im}[Y_{\mathrm{in,upper}}] = 0$, the resonant frequency can be determined as:

$$2\pi C_{\mathrm{v2}} f_{\mathrm{upper}} + Y_1 \tan\left(\frac{\pi f_{\mathrm{upper}} L_1}{v_p}\right) = 0 \tag{9}$$

Similarly, for the short stub, as shown in fig. 3(a), a series structure of a inductor and a varactor diode is used to replace the short stub. The specific circuit diagram is shown in fig. 4(b).

For this series structure consisting of an inductor and a varactor diode, the input impedance can be expressed:

$$Y_{\mathrm{in,lower}} = Y_1 \frac{Y_{s1} + jY_1 \tan\dfrac{\theta_1}{2}}{Y_1 + jY_{s1} \tan\dfrac{\theta_1}{2}} \tag{10}$$

where

$$Y_{sl} = \frac{j\omega C_{\mathrm{v1}}}{1-\omega^2 L_x C_{\mathrm{v1}}} \tag{11}$$

For the resonance condition of $\mathrm{Im}[Y_{\mathrm{in,lower}}] = 0$, the resonant frequency can be determined:

$$2\pi f_{\mathrm{lower}} C_{\mathrm{v1}} + Y_1 (4\pi^2 f^2{}_{\mathrm{lower}} L_x C_{\mathrm{v1}}) \tan\left(\frac{\pi f_{\mathrm{lower}} L_1}{v_p}\right) = 0 \tag{12}$$

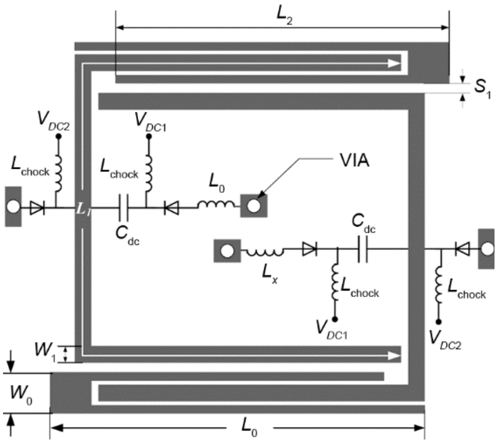

Figure 5. Configuration of the proposed filter

The overall design of the proposed resonator is shown in fig. 4(a). It can be observed from eqs. (9) and (12), f_{upper} is determined by transmission line L_1 and varactor diode C_{v2}, while f_{lower} is determined by L_1 , C_{v1}, and L_x. Thus, if the parameters of the transmission line L_1 and the inductor L_x are fixed, the resonance frequency f_{upper} and f_{lower} will be determined only by the capacitance values of the respective varactor diodes. So the two frequencies can be tuned independently of each other.

To verify the previous analysis, full-wave electromagnetic simulation was carried out by using HFSS, and an experimental reconfigurable tri-band BPF was designed and fabricated. The configuration of this design is shown in fig. 5, it comprises two reconfigurable tri-band resonators which are meandered to reduce the filter size. The silicon varactor diodes used in this design are SMV1408 from Skyworks. In order to obtain stable DC bias voltages, RF DC blocking capacitors are also used in this design.

The substrate of this design has a thickness of 0.8 mm and a relative dielectric constant of 2.33, the total size is less than 12 mm × 19 mm, or $0.12\lambda_g$ by $0.09\lambda_g$, where λ_g denotes the guided wavelength on the substrate at the central of the first passband frequency. The dimensions are selected as follows (in millimeters): L_0 = 19.7, L_1 = 42.3, L_2 = 17.6, W_0 = 2.3, W_1 = 0.9, S_1 = 0.52. The length of the half-wavelength microstrip line, L_1, is always fixed in all the simulation and experiment process. The value of the lumped inductance L_x has also remained fixed.

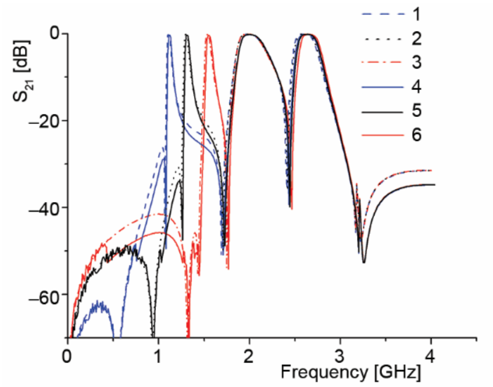

Figure 6. Simulated S_{21} against V_{DC1};
1 – simulated V_{DC1} = 0.2 V, 2 – simulated V_{DC1} = 1.6 V, 3 – simulated V_{DC1} = 3.5 V, 4 – measured V_{DC1} = 0.2 V, 5 – measured V_{DC1} = 1.6 V, 6 – measured V_{DC1} = 3.5 V (for color image see journal web site)

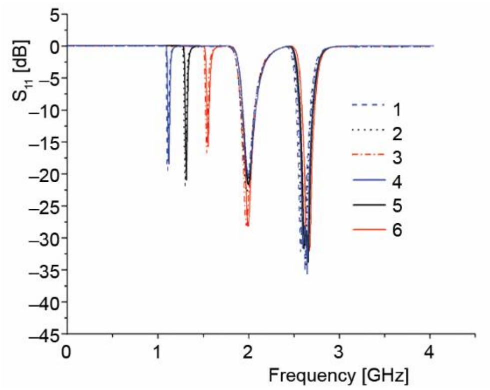

Figure 7. Simulated S_{11} against V_{DC1};
1 – measured V_{DC2} = 0.2 V, 2 – measured V_{DC2} = 1.6 V, 3 – measured V_{DC2} = 3.5 V, 4 – measured V_{DC2} = 0.2 V, 5 – measured V_{DC2} = 1.6 V, 6 – measured V_{DC2} = 3.5 V (for color image see journal web site)

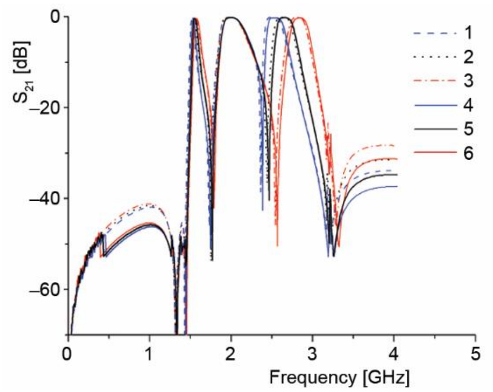

Figure 8. Simulated S_{21} against V_{DC2};
1 – simulated V_{DC2} = 0.2 V, 2 – simulated V_{DC2} = 1.6 V, 3 – simulated V_{DC2} = 3.5 V, 4 – measured V_{DC2} = 0.2 V, 5 – measured V_{DC2} = 1.6 V, 6 – measured V_{DC2} = 3.5 V (for color image see journal web site)

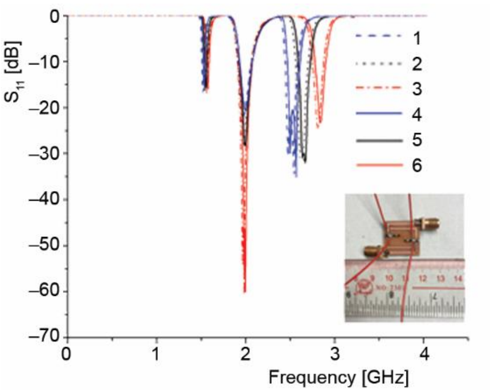

Figure 9. Simulated S_{11} against V_{DC2};
1 – simulated V_{DC2} = 0.2 V, 2 – measured V_{DC2} = 1.6 V, 3 – measured V_{DC2} = 3.5 V, 4 – measured V_{DC2} = 0.2 V, 5 – measured V_{DC2} = 1.6 V, 6 – measured V_{DC2} = 3.5 V (for color image see journal web site)

Figures 6-9 describe the simulation and measured results of the filter, which has one fixed passband and two controllable passbands. In this case, the bias voltage of the varactor diode V_{DC2} is fixed at 0.5 V, whereas the bias voltage V_{DC1} varies from 0.2 V to 3.5 V. As seen from fig. 6, the second passband frequency f_{odd} is constant at 2.0 GHz and the third passband frequency f_{upper} is almost fixed at 2.65 GHz, respectively. Meanwhile, the first passband frequency f_{lower} is controlled with the bias voltage V_{DC1}. As the bias voltage V_{DC1} varies, the first passband frequency f_{lower} can be tuned simultaneously. From the results, it can be seen that the first passband frequency f_{lower} can be tuned from 1.12 GHz to 1.56 GHz. Figure 7 shows the corresponding S_{11} simulation and measurement results in this case.

Figure 8 shows the continuous tuning of the third frequency. In this case, the bias voltage of the varactor diode V_{DC1} is fixed at 0.5 V, meanwhile the bias voltage V_{DC2} varies from 0.2 V to 3.5 V. As seen from this figure, the first passband frequency f_{lower} is almost constant at 1.56 GHz and the second passband frequency f_{odd} is fixed at 2.0 GHz. Meanwhile, the third passband frequency f_{upper} can be tuned with the help of the bias voltage V_{DC2}. As the bias voltage V_{DC2} varies, the third passband frequency f_{upper} can be tuned from 2.50 GHz to 2.84 GHz. Figure 9 shows the corresponding S_{11} simulation and measurement results in this case.

Conclusion

In this paper, a reconfigurable tri-mode resonator and its application to tri-band BPF have been demonstrated. Both the theoretical analysis and experimental results are presented to validate the proposed structure. The experimental results are in agreement with the theoretical analyses. For the proposed filter, it has two independent tunable frequency bands. The measured center frequency f_{lower} can be tuned from 1.12-1.56 GHz, featuring the fractional tuning range of 32.8%, meanwhile f_{upper} can be tuned from 2.50-2.84 GHz, featuring the fractional tuning range of 12.73%. Moreover, the measured fractional bandwidth are changed from 4.46% to 4.57% and 8.45 to 8.8% for the lower and upper passbands, respectively. The agreement between simulation and measurement is reasonable.

Across all the tuning range, the filter has almost constant fractional bandwidths and passband shapes. For each tuning state, measured return loss is greater than 15 dB and insertion loss varies from 2.1 to 2.8 dB. Besides, the filter has a very compact size of 0.12 λ_g × 0.08 λ_g. Furthermore, transmission zeros are realized near the passband frequencies, which offers high selectivity of the filter. The proposed filter design method can be used to selectable multimode or multiband applications.

Nomenclature

C – capacitor, [F]
f – frequency, [Hz]
L – inductance, [H]

Greek symbol

λ – wavelength, [m]

References

[1] Chen, Z. H., *et al.*, Dual-band Reconfigurable Bandpass Filter with Independently Controlled Passbands and Constant Absolute Band-widths, *IEEE Microwave And Wireless Components Letters*, *26* (2016), 2, pp. 92-94

[2] Sedighi, S. M., *et al.*, Tunable Dual-band Bandpass Filter for Multi-standard Applications, *Aeu-International Journal of Electronics and Communications, 5* (2019), 8, 152885

[3] Yang, Z. J., *et al.*, A Balanced Dual-Band Bandpass Filter with Independently Tunable Differential-mode Frequencies, *International Journal of RF and Microwave Computer-Aided Engineering, 28* (2018), 6, pp. 1-6

[4] Amjad, I., *et al.*, Dual-Band Half Mode Substrate Integrated Waveguide Filter With Independently Tunable Bands, *IEEE Transactions On Circuits And Systems II: Express Briefs, 67* (2020), 2, pp. 285-289
[5] Zhang, S. X., *et al.*, Design of Tri-band Bandpass Filter with Tunable Lower Passband, *Proceedings*, IEEE International Workshop On Electromagnetics: Applications and Student Innovation Competition (iWEM), Nanjing, China, 2016, pp. 1-3
[6] Du, X., *et al.*, Novel Tri-band Bandpass Filter with One High Selective Tunable Passband, *Microwave and Optical Technology Letters*, *59* (2017), 6, pp. 1464-1468
[7] Kingsly, S. M., *et al.*, Multi-Band Reconfigurable Microwave Filter Using Dual Concentric Resonators, *International Journal of RF and Microwave Computer-Aided Engineering*, *28* (2018), 6, e21290
[8] Zhang, F., *et al.*, A Compact Tri-Band Microstrip Filter with Independently Tunable Passbands and High Selectivity, *IEICE Electronics Express,16* (2019), 22, pp. 1-3
[9] Wang, Z. J., *et al.*, Dual−/Triple-wideband Microstrip Bandpass Filter Using Independent Triple-mode Stub-loaded Resonator, *Microwave and Optical Technology Letters, 60* (2018), 1, pp. 56-64
[10] Zhang, S., *et al.*, A Novel Triple-Band Bandpass Filter Based on Equilateral Triangle Substrate Integrated Waveguide, *Microwave and Optical Technology Letter, 60* (2018), 3, pp. 575-578
[11] Li, X. K., *et al.*, Quad- and Sext-band Bandpass Filter Based on Multimode Resonator Utilizing SIRs-loaded Tapered-line, *Microwave and Optical Technology Letters, 60* (2018), 3, pp. 650-654
[12] Sung, Y., Simple Quad-Band Bandpass Filter Implemented on a 50-Ω microstrip line, *Microwave and Optical Technology Letters*, *62* (2020), 1, pp. 100-107
[13] Rahman, M. U., *et al.*, A Compact Tri-Band Bandpass Filter Utilizing Double Mode Resonator with 6 Transmission Zeros, *Microwave and Optical Technology Letters*, *60* (2018), 7, pp. 1767-1771
[14] Wang, J., *et al.*, A 2.4/3.5/5.2/5.8-GHz Quad-band BPF Using SLRs and Triangular Loop Resonators, *Electronics Letters, 54* (2018), 5, pp. 299-301
[15] Xu, J. X., *et al.*, Compact Tri-band Bandpass Filter with Controllable Frequencies, *Microwave and Optical Technology Letter, 58* (2016), 3, pp. 573-577

Paper submitted: April 11, 2021
Paper revised: July 6, 2021
Paper accepted: July 27, 2021